

The University of Akron IdeaExchange@UAkron

College of Polymer Science and Polymer Engineering

1-21-2006

Coupling Between Lysozyme and Trehalose Dynamics: Microscopic Insights from Molecular-Dynamics Simulations

Taner E. Dirama

Joseph E. Curtis

Gustavo A. Carri

University of Akron Main Campus, gac@uakron.edu

Alexei P. Sokolov

Please take a moment to share how this work helps you [through this survey](#). Your feedback will be important as we plan further development of our repository.

Follow this and additional works at: http://ideaexchange.uakron.edu/polymer_ideas

 Part of the [Polymer Science Commons](#)

Recommended Citation

Dirama, Taner E.; Curtis, Joseph E.; Carri, Gustavo A.; and Sokolov, Alexei P., "Coupling Between Lysozyme and Trehalose Dynamics: Microscopic Insights from Molecular-Dynamics Simulations" (2006). *College of Polymer Science and Polymer Engineering*. 3.

http://ideaexchange.uakron.edu/polymer_ideas/3

This Article is brought to you for free and open access by IdeaExchange@UAkron, the institutional repository of The University of Akron in Akron, Ohio, USA. It has been accepted for inclusion in College of Polymer Science and Polymer Engineering by an authorized administrator of IdeaExchange@UAkron. For more information, please contact mjon@uakron.edu, uapress@uakron.edu.

Coupling between lysozyme and trehalose dynamics: Microscopic insights from molecular-dynamics simulations

Taner E. Dirama

Department of Polymer Science, The University of Akron, Akron, Ohio 44325-3909

Joseph E. Curtis

National Institute of Standards and Technology, Gaithersburg, Maryland 20899

Gustavo A. Carri^{a)} and Alexei P. Sokolov

Department of Polymer Science, The University of Akron, Akron, Ohio 44325-3909

(Received 26 August 2005; accepted 29 November 2005; published online 17 January 2006)

We have carried out molecular-dynamics simulations on fully flexible all-atom models of the protein lysozyme immersed in trehalose, an effective biopreservative, with the purpose of exploring the nature and extent of the dynamical coupling between them. Our study shows a strong coupling over a wide range of temperatures. We found that the onset of anharmonic behavior was dictated by changes in the dynamics and relaxation processes in the trehalose glass. The physical origin of protein-trehalose coupling was traced to the hydrogen bonds formed at the interface between the protein and the solvent. Moreover, protein-solvent hydrogen bonding was found to control the structural relaxation of the protein. The dynamics of the protein was found to be heterogeneous; the motions of surface and core atoms had different dependencies on temperature and, in addition, the surface atoms were more sensitive to the dynamics of the solvent than the core atoms. From the solvent perspective we found that the dynamics near the protein surface showed an unexpected enhanced mobility compared to the bulk. These results shed some light on the microscopic origins of the dynamical coupling in protein-solvent systems. © 2006 American Institute of Physics. [DOI: 10.1063/1.2159471]

I. INTRODUCTION

The observation of large concentrations of trehalose in cells undergoing anhydrobiosis has motivated numerous studies of this compound.¹ The main focus of these studies has been to understand the molecular mechanisms responsible for the enhanced effectiveness of trehalose in the biopreservation of living organisms.²⁻⁵ One important component of these systems is proteins; thus, protein-trehalose mixtures have been studied extensively.⁴⁻⁷ Since the denaturation of biological agents is a dynamical phenomenon,⁵ the efforts have concentrated in understanding the dynamics of protein-trehalose systems at different length and time scales.

It is well known that proteins have to go through a series of conformational changes in order to carry out their biological functions. It is evident from the classical example of binding of oxygen to myoglobin that structural fluctuations must be involved in the binding mechanism since high-resolution x-ray studies of the protein structure do not reveal any path by which dioxygen can reach the heme group from the solvent directly.⁸ In fact, it has been shown experimentally that the biological functions of proteins are affected by the structural fluctuations among the conformational substates.⁹ It was suggested that the solvent surrounding the protein could play an essential role in the activation of these fluctuations.¹⁰ Therefore, one can decrease the biological

function of the protein by embedding it in viscous solvents which suppress the fluctuations between conformational substrates.^{2,11}

The protein dynamical transition, defined as the temperature where large-amplitude anharmonic motions are activated and start to dominate the dynamics of the protein, has been suggested as to originate from the solvent glass transition.^{12,13} Experimental^{2,14} and simulation¹⁵ studies show that the protein motion below the dynamical transition is inhibited by high solvent viscosity. It traps the protein in long-living conformations such that the conformational transitions necessary for biological function or denaturation are strongly repressed. This slowdown is a consequence of the solvent which controls the motions of the protein through the coupling of the protein and solvent dynamics.¹⁶⁻¹⁸ This coupling may explain how biopreservative solvents function: the protein becomes "slaved" to the solvent molecules that suppress its dynamics, resulting in a retardation of the denaturation process or a slowing down of its biological function.

The primary goal of this article is to contribute to the understanding of the dynamics of proteins immersed in trehalose which has been reported to be the most effective protecting agent by means of functional recovery.¹⁹ For this purpose we employ the model protein lysozyme. We constructed our model system without water molecules for the purpose of modeling the system in freeze-dried form where water content is minimal.²⁰ As a first approximation we assumed that the hydration shell is entirely removed and leaves its study for a future publication. Using molecular-dynamics (MD)

^{a)}Author to whom correspondence should be addressed. Electronic mail: gac@uakron.edu

simulations, we studied the protein dynamics and examined the extent of the dynamical coupling between the protein and the solvent. The relevance of hydrogen bond interactions for the dynamics of the protein and its dynamical coupling with the solvent was also explored. Additionally, we investigated the possible routes through which the dynamics of the protein couples to the dynamics of the solvent.

This article is organized as follows. Section II describes the details of the simulation protocol. The results of our study are presented in Sec. III. Particularly, the dynamical coupling of trehalose and lysozyme is shown and a correlation between the behavior of hydrogen bonds and the dynamics of the protein is presented. We discuss our results in Sec. IV. The conclusions of this work are given in Sec. V followed by the appropriate acknowledgments.

II. SIMULATION PROTOCOL

The AMBER molecular-dynamics package²¹ with ff99 (Ref. 22) and general amber force field (GAFF) (Ref. 23) force fields was used in this study to model lysozyme and trehalose, respectively. The electrostatic potentials on atom surfaces of trehalose in the crystalline state²⁴ were calculated using the software package GAUSSIAN 03 (Ref. 25) with (ground state) Hartree-Fock method and 6-31G basis set. Point charges on the atomic nuclei were then fitted by restrained electrostatic potential (RESP). The structure of hen egg white lysozyme was obtained from the Protein Data Bank (193L).

Rectangular periodic boundary conditions were used. Long-range electrostatic interactions were calculated using the particle-mesh Ewald (PME) method, while van der Waals interactions were calculated using the 6-12 Lennard-Jones potential. The cutoff distance for nonbonded van der Waals interactions was set to 8 Å. However, in the case of electrostatic interactions this cutoff is used for the evaluation of Ewald's standard direct sum; corrections are taken into account via the reciprocal sum. The hydrogen bonds in this all-atom potential function are represented by a balance between electrostatic and van der Waals interactions. Random initial velocities were assigned to all atoms after minimization of the initial structure. The equations of motion were integrated using leapfrog Verlet algorithm with a step size of 1 fs. Constant temperature and pressure were satisfied by a weak-coupling algorithm.²⁶

A simulation box of trehalose was preequilibrated at 300 K (Ref. 27) and the energy-minimized structure of lysozyme was placed at the center. The trehalose molecules within 2 Å from the surface of lysozyme were removed from the simulation box. The resulting protein-solvent mixture with 283 trehalose molecules was then equilibrated first under constant volume and temperature conditions for 50 ps and then under isothermal-isobaric conditions for 300 ps at 500 K and 0.1 MPa. Afterward, the simulation box was annealed to 300 K at a rate of 0.1 K/ps. During this stage of the equilibration we put harmonic restraints on the protein atoms to maintain the native structure. Following an additional equilibration at 300 K for 2.7 ns where the restraints were removed, the data collection run was performed in

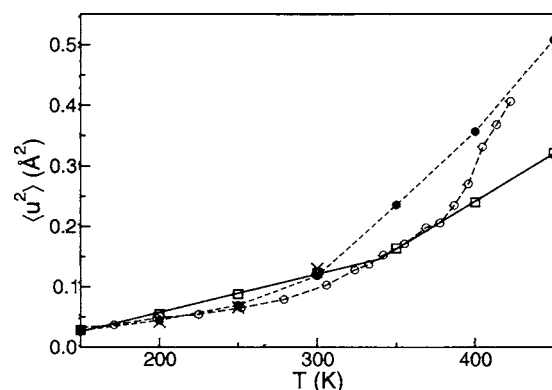


FIG. 1. Temperature dependence of the mean-square displacement of the hydrogen atoms in lysozyme immersed in trehalose (\square), in the surrounding trehalose molecules (\bullet), pure trehalose molecules (Ref. 27) (\times), and experimental data for pure trehalose from Ref. 30 (\circ). The continuous lines are linear fits to the low- and high-temperature behaviors of lysozyme. Mean-square displacement values were calculated for 0.8 ns of simulation.

isothermal-isobaric conditions for 2 ns and coordinate sets were saved for every 0.1 ps intervals for subsequent analysis. For the simulations at 250, 200, and 150 K the system was first annealed to 50 K below the current temperature at a cooling rate of 0.1 K/ps followed by an equilibration in the *NPT* ensemble at this temperature before the data collection run. At temperatures higher than 300 K, the system was equilibrated at the higher temperature followed by the data collection. The trajectories for pure trehalose, which are used to compare the dynamics of the protein with the pure solvent, were taken from our previous work.²⁷

III. RESULTS

The dynamical transition temperature (T_d) is usually defined as the temperature at which mean-square displacement of atoms ($\langle u^2 \rangle$) in the protein exhibits a sharp change in its temperature dependence.²⁸ This working definition of T_d is equivalent to the saying that large-amplitude anharmonic motions are activated and start to dominate the dynamics of the protein. We chose the hydrogen atoms to compute T_d and other dynamic quantities such as $\langle u^2 \rangle$ for two reasons. First, they are distributed throughout both the protein and solvent molecules, thus enabling us to probe the dynamics of all molecules consistently. Second, experimental data from incoherent neutron spectroscopy are dominated by hydrogen atoms, and thus the hydrogens are a useful probe that allows the validation of our simulation methodology. Consequently, we can compare our results with the experimental data directly. T_d is computed from the plot of $\langle u^2 \rangle$ versus temperature as the intercept between two straight lines: the first line is a fit of $\langle u^2 \rangle$ as a function of temperature at low temperatures and the second line is the same fit but at high temperatures. Figure 1 shows $\langle u^2 \rangle$ for the *hydrogen* atoms in lysozyme as a function of temperature. $\langle u^2 \rangle$ was obtained after averaging over 800 ps of the 2 ns data set using multiple time origins. A straight line was fitted to the first four data points at low temperatures. In this region $\langle u^2 \rangle$ increases linearly with temperature up to 300 K, whereas, above this temperature, $\langle u^2 \rangle$ escalates nonlinearly, thus indicating that

there are two distinct dynamical regimes, as has been observed experimentally in various solvated proteins.^{4,5,29} In the trehalose-lysozyme system studied in this work the onset of anharmonic behavior was found to be ~ 350 K which is below the glass transition temperature of trehalose. Previous neutron-scattering⁴ and Mössbauer spectroscopy⁵ measurements of myoglobin (MbCO) at similar time resolutions did not show a clear indication of the dynamical transition because $\langle u^2 \rangle$ data were reported for temperatures below 300 K.

Figure 1 also shows $\langle u^2 \rangle$ for the hydrogen atoms in trehalose and experimental data for pure trehalose (empty circles).³⁰ $\langle u^2 \rangle$ for trehalose obtained from the simulation displays a change in dynamics at temperatures close to 300 K which is below the glass transition temperature.²⁷ This change in dynamics of a dehydrated trehalose glass agrees with the experimental results,³⁰ thus validating our simulation protocol. Analysis of the experimental data for pure trehalose shows three temperature regimes. The first regime is below 300 K, the second regime is between 300 and 390 K, and the last regime is above 390 K. The experimental T_g of trehalose is ~ 390 K. Since the change in the temperature dependence of $\langle u^2 \rangle$ of trehalose around 300 K occurs deep in the glassy state, it should be related to a secondary relaxation and not to a translational diffusion of trehalose molecules. It is known that pure trehalose has secondary relaxation active in the glassy state.³¹ According to dielectric studies,³¹ this secondary relaxation process is strongly stretched and should reach our nanosecond time window at temperatures $T \sim 330$ – 390 K. This agrees well with the results of the simulations and neutron-scattering studies³⁰ (Fig. 1). The onset of the protein dynamical transition in trehalose occurs over a much broader temperature range than that observed of hydrated protein powders or proteins in glycerol.^{4,5,29} This onset of anharmonic behavior of the protein occurs above the 300 K transition temperature of trehalose, suggesting that some softening of the glass is required before the protein can undergo the dynamical transition. In the protein-trehalose system the activation of significant conformational motions of the solvent (the secondary relaxation that appears as a strong increase in $\langle u^2 \rangle$) allows for the onset of anharmonic motions of the protein far below the T_g of the solvent.

The protein dynamical transition is dependent on the surrounding solvent molecules.^{4,14,17,32–34} The mechanism by which the solvent affects the protein dynamics can be explained through the coupling between the protein and solvent dynamics. This coupling is often called “slaving” because the dynamics of the protein is controlled by (i.e., is a slave of) the dynamics of the solvent as demonstrated by various experimental^{16,35–38} and MD simulation^{34,39,40} studies. In this work, the incoherent intermediate scattering function, $S(q, t)$, and dynamic structure factor, $S(q, \nu)$, for the (pure) solvent and the protein atoms were used to probe the existence and the extent of the dynamical coupling.

The dynamics of the solvent and the protein were compared using $S(q, t)$, which was calculated as explained elsewhere.⁴¹ $S(q, t)$ for lysozyme was computed in two different ways. First, we computed $S(q, t)$ considering all hydrogen atoms and, second, we excluded those hydrogens belonging to methyl groups. The methyl groups are unique in

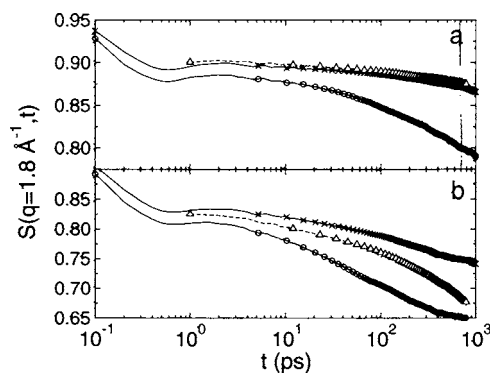


FIG. 2. Incoherent intermediate scattering function of the hydrogen atoms in lysozyme: with (○) and without (×) methyl hydrogen atoms, and pure trehalose molecules (△) at (a) 200 K and (b) 300 K.

the sense that their motions in protein powders are activated at temperatures as low as 100 K,⁴² while the rest of the protein has predominantly harmonic vibrations in the nanosecond time scale. Thus the methyl group hydrogens have distinct dynamical behavior and their incorporation into the calculation of the dynamical observables may complicate the interpretation of the structural relaxation of the protein.⁴² The emerging hypothesis is that the structural relaxation of the protein is related to the activation of modes involving large-scale motions of secondary structural elements. Since the dynamics of methyl protons occur on this moving framework, the inclusion of their contribution to the relaxation process may overwhelm or complicate the analysis of the underlying physical processes. Figure 2 illustrates how the dynamics of lysozyme relates to the dynamics of pure trehalose. At 200 K, Fig. 2(a), when the dynamics of methyl-group hydrogens are neglected, $S(q, t)$ for lysozyme and trehalose are very similar indicating a strong correlation in the structural relaxation of lysozyme and trehalose in the 1 ns time window. This result implies that, on average, practically all the modes with characteristic time scales between 1 ps and 1 ns are strongly coupled. The dynamical coupling at this low temperature could be due to the fact that the system is deep in the glassy state where protein atoms could be trapped in the cage created by the surrounding solvent molecules. At higher temperatures, as shown in Fig. 2(b), $S(q, t)$ for trehalose decays faster than $S(q, t)$ for lysozyme.

In order to evaluate the conformity between experiments and our simulations, we compared the dynamic structure factor, $S(q, \nu)$, obtained from MD simulations to experimental neutron-scattering spectra for lysozyme in trehalose in Fig. 3.¹⁸ The experimental resolution was taken into account by convoluting the $S(q, t)$ in the time domain with a Gaussian function with full width at half maximum (FWHM) of $500 \mu\text{eV}$ which corresponds to an energy resolution of $210 \mu\text{eV}$. The details of the calculation have been explained elsewhere.⁴¹

We compare the results from the simulations with the experimental data in Fig. 3. Since the experimental $S(q, \nu)$ has arbitrary units the simulation data (lines) were scaled and shifted *vertically* to maximize the agreement between both results. Different values of the scaling parameters and vertical shifts were used for the data obtained at 150 and 300 K.

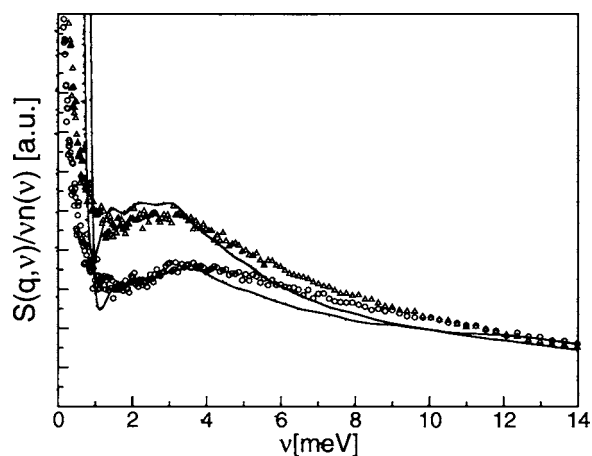


FIG. 3. Dynamic structure factor for lysozyme in trehalose from MD simulation (lines) and from neutron-scattering spectra (symbols) from Caliskan *et al.* (Ref. 18). The upper and bottom curves/symbols correspond to temperatures of 300 and 150 K, respectively. $n(\nu)=[\exp(h\nu/kT)-1]^{-1}$ is the Bose factor.

A good quantitative agreement is observed between our simulations and the experimental data at 150 and 300 K. The presence, location, and temperature dependence of the inelastic boson peak is captured by our simulations.

Reproducing $S(q, \nu)$ enables us to study the coupling of the protein and the solvent dynamics in the frequency domain. For this purpose we present $S(q, \nu)$ for lysozyme in trehalose and pure trehalose for a scattering vector of magnitude 1.8 \AA^{-1} and temperatures equal to 200, 300, and 400 K in Fig. 4. Note that the spectral shapes of $S(q, \nu)$ for lysozyme and pure trehalose follow one another very closely. The boson peak is clearly observed for both systems at 200 and 300 K while, at 400 K, it appears as a shoulder due to the intensity of quasielastic scattering (QES) which increases with temperature and overlaps with the contribution arising from inelastic scattering. The physical origin of the boson peak for glassy systems as well as proteins is still a subject of discussion.⁴³ In order to illustrate the similar dynamics of the protein and the solvent, we plot the frequency of the boson

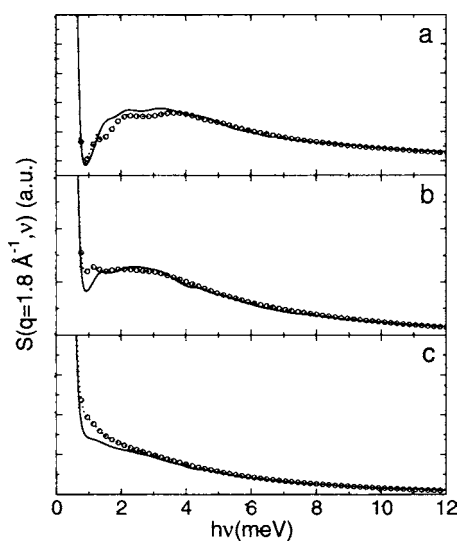


FIG. 4. Dynamic structure factor for pure trehalose (○) and lysozyme (continuous line) at (a) 200 K, (b) 300 K, and (c) 400 K.

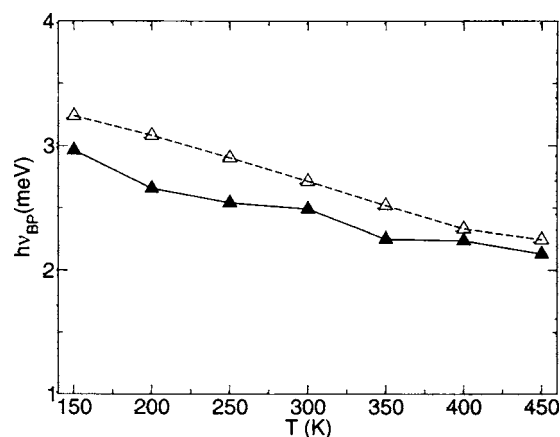


FIG. 5. Temperature dependence of the frequency of the boson peak from MD simulation. Lysozyme (▲) and pure trehalose (△).

peak (ν_{BP}) as a function of temperature for both systems in Fig. 5. ν_{BP} was extracted from the simulation data using the extrapolation formula

$$S(q, \nu) = \frac{A\nu_0}{\nu_0^2 + \nu^2} + B \exp\left\{-\frac{[\ln(\nu/\nu_{BP})]^2}{2[\ln(W/\nu_{BP})]^2}\right\} \quad (1)$$

that comprises two terms: the first one approximates the QES part with a Lorentzian function of width ν_0 and height A/ν_0 , whereas the second term (long-normal function) fits the boson peak of width W .⁴⁴ Figure 5 shows a similar temperature dependence of the frequencies of the boson peak for lysozyme and pure trehalose from 150 to 450 K, implying that the low-frequency collective vibrations are coupled, in agreement with results from Raman spectroscopy.¹⁸ This result, in conjunction with the analysis of $S(q, t)$ depicted in Fig. 2, implies that our simulation protocol is also capable of reproducing the coupling of the protein and solvent dynamics.

Since the protein-solvent interactions occur at the protein-solvent interface, this region carries crucial information regarding the microscopic origins of the coupling between the protein and solvent dynamics. The protein atoms comprising the protein side of the interface are affected by the solvent molecules more strongly than the core atoms. Therefore, the dynamics of the surface and core atoms of the protein are likely to be influenced by the solvent differently. The hydrogen atoms in the protein that are the closest to trehalose atoms were determined as surface atoms and the rest were considered as core atoms. This definition resulted in 440 surface and 537 interior hydrogen atoms. The comparison of their dynamics as measured by $S(q, t)$ along with the one of pure trehalose is shown in Fig. 6.

Let us first evaluate the dynamics of the protein and the solvent molecules prior to analyzing the dynamics of the surface and core separately. At 200 K, Fig. 6(a), the atoms of trehalose are trapped in smaller cages than the protein atoms, as manifested by higher values of $S(q, t)$ at short times. Additionally, the secondary relaxation in trehalose is slower than in lysozyme. The reason why trehalose appears to be less mobile than lysozyme will be elucidated in the Discussion section. At 300 K, trehalose shows a secondary decay

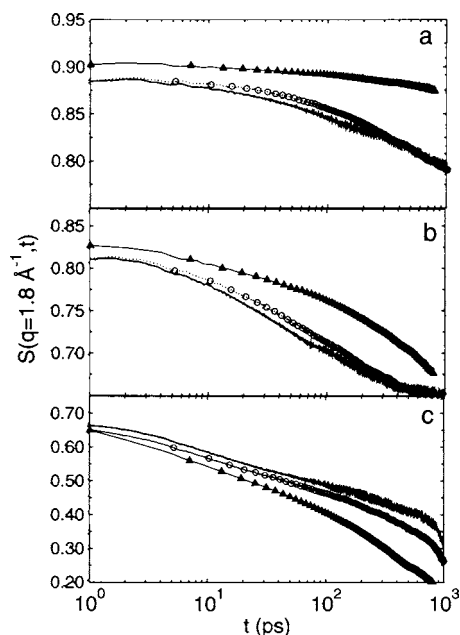


FIG. 6. Incoherent intermediate scattering function for pure trehalose (\blacktriangle), and surface (\circ) and core (continuous line) hydrogen atoms in lysozyme at (a) 200 K, (b) 300 K, and (c) 400 K.

similar to lysozyme. An important observation can be made at this point: at 200 K, when the dynamics of trehalose is relatively slower than the one of lysozyme; the dynamics of protein atoms on the surface is slower than the core atoms while, at 400 K [Fig. 6(c)], when trehalose is more mobile than lysozyme, the protein surface has relatively faster dynamics than the core. At intermediate temperatures, i.e., 300 K, when the dynamics of the solvent approaches that of the protein, the surface and the core protein atoms show nearly the same dynamical behavior. These results indicate that the surface of the protein is more sensitive to dynamics of the solvent than the interior.

Let us now explore the effect of the protein on the dynamics of the surrounding solvent which is often overlooked in studies of protein-solvent systems. Previous studies on protein-water⁴⁵⁻⁴⁷ and protein-glycerol⁴¹ systems demonstrated that the dynamics of solvent molecules near the surface of the protein is more restricted than in the bulk.⁴⁶ The restricted mobility of water near the protein surface has been ascribed mainly to the decrease in the dimensionality of the space near the interface.⁴⁶ Additionally, the restricted mobility near the protein was suggested to be a universal behavior for protein-solvent systems.⁴⁶ In order to evaluate the validity of this observation in the case of trehalose we calculated $S(q, t)$ and $\langle u^2 \rangle$ for the hydrogen atoms in trehalose as a function of the distance from the surface of lysozyme. $S(q, t)$ is shown in Fig. 7. The distance to the surface was computed following the work of Makarov *et al.*⁴⁶ Average positions of solvent hydrogen atoms were sorted into six shells with respect to the distance from their nearest protein atom. The first shell comprised the hydrogens within a distance of 4.5 Å from the protein surface, the following four shells were created with a thickness of 2.5 Å, and the last shell consisted of hydrogens between 14.5 and 24.5 Å from the surface of the protein. Figure 7 shows that the initial decay

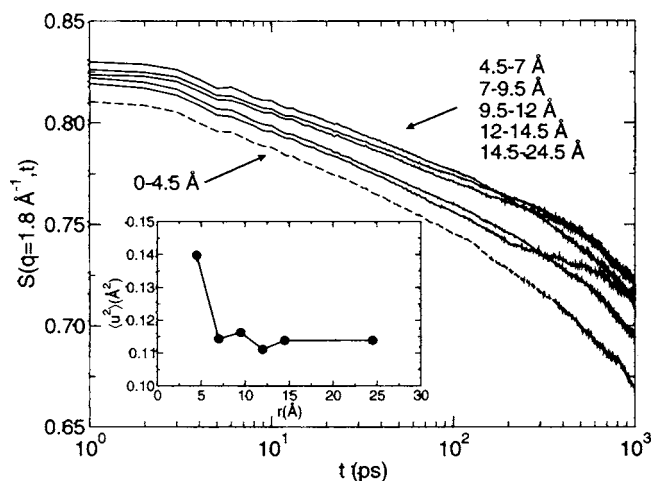


FIG. 7. Incoherent intermediate scattering function for trehalose molecules within 0–4.5 Å (dashed line) and larger distances (continuous lines) from the surface of lysozyme at 300 K. Inset shows the mean-square displacement of the hydrogen atoms in trehalose as a function of the distance from the surface of lysozyme at 300 K.

of $S(q, t)$ is larger for the first shell of solvent than for the other shells, suggesting that trehalose is more mobile near the protein surface than in the bulk. This is confirmed by $\langle u^2 \rangle$ shown in the inset. $\langle u^2 \rangle$ increases from the bulk value as one approaches the protein surface. This result is the opposite of what has been observed in the previous studies. The reason for this unexpected behavior will be clarified later in the Discussion section. The same trend shown in Fig. 7 was also observed at temperatures 150, 200, and 250 K but this behavior is reversed at higher temperatures, e.g., 550 K.

Among various kinds of interactions in molecular systems, hydrogen bonds are particularly important in the dynamics of proteins.⁴⁸ Proteins contain many polar groups in the backbone as well as in the side groups that can form intramolecular and intermolecular hydrogen bonds. Since trehalose is a very good candidate for forming hydrogen bonds with proteins, it is expected that the dynamics of such a protein-solvent system will be greatly influenced by the formation of the hydrogen bonds at the protein-solvent interface. The hydrogen bonding behavior was evaluated using geometric criteria which were based on the distance between the donor and the acceptor oxygen atoms, and the angle formed by the donor oxygen, the acceptor hydrogen, and the acceptor oxygen atoms.⁴⁹ The cutoff distance between oxygen atoms was set to 3.4 Å and the cutoff for the angle was set to 120°. Based on these criteria we implemented a hydrogen bond correlation function analysis where the hydrogen bonds were characterized by hydrogen bond correlation function using the following equation:

$$c(t) = \frac{\langle h(t)h(0) \rangle}{\langle h \rangle}, \quad (2)$$

where $h(t)$ is hydrogen bond population operator which is equal to one when a donor-acceptor pair satisfies the hydrogen bond criteria at time t and it is zero otherwise. $c(t)$ yields the probability that a random donor-acceptor pair that is hydrogen bonded at time zero is still bonded at time t . The decay of $c(t)$, and its characteristic time constant, $\tau_{R,HB}$, can

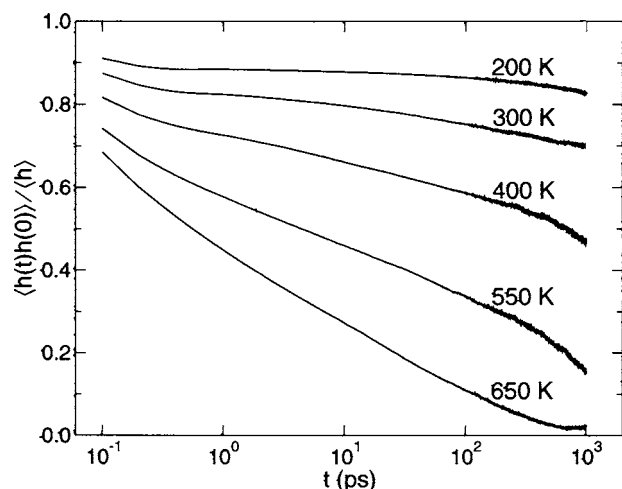


FIG. 8. Hydrogen bond correlation function for the hydrogen bonds between trehalose and lysozyme at five temperatures.

be used to quantify the effectiveness of the hydrogen bond network formed between the protein and solvent molecules.

Hydrogen bond correlation functions for the hydrogen bonds between lysozyme and trehalose molecules are shown in Fig. 8 for wide range of temperatures: 200, 300, 400, 550, and 650 K. At temperature 400 K and below, there is a clear indication of an initial decay. Based on an earlier study by Tarek and Tobias³⁹ on the analysis of the hydrogen bond dynamics this decay corresponds to rotation and libration of the protein and the solvent atoms. These motions allow the formation of hydrogen bonds with lifetimes shorter than 1 ps. On the other hand, at higher temperatures the initial decay is merged with a secondary decay, also seen at lower temperatures, which is a consequence of the long-living hydrogen bonds. Since the relaxation of the protein-solvent hydrogen bonding network is required for the structural relaxation of the protein,³⁹ the secondary decay in the correlation function has important implications on the protein dynamics.

In order to study the relationship between the structural relaxation of the protein and the hydrogen bond network we determined the relaxation time of the *long-living* hydrogen bonds ($\tau_{R,HB}$) and the relaxation time of the intermediate scattering function ($\tau_{R,ISF}$) at a set of temperatures. In both cases τ_R was obtained from stretched exponential fits to the data.⁴¹ Figure 9 shows the cross correlation of $\tau_{R,HB}$ and $\tau_{R,ISF}$. There is a power-law relationship between both relaxation times with exponent and prefactor equal to 0.8 and 5.2, respectively. This result is consistent with previous findings for a glycerol-lysozyme system,⁴¹ and indicates that the relaxation of the protein-solvent hydrogen bond network at the protein-solvent interface dominates the structural relaxation of the entire protein, at least in the time window accessible to our MD simulation study.

IV. DISCUSSION

The protein dynamical transition typically observed in solvated and hydrated proteins is captured by our MD simulation of lysozyme in trehalose, as illustrated by Fig. 1. Previous experimental studies have not reported a protein dynamical transition in trehalose possibly due to the

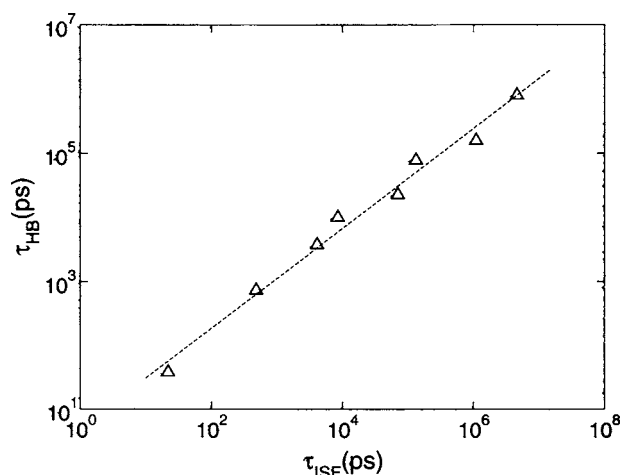


FIG. 9. Plot of the relaxation time for the hydrogen bonds between the protein and the solvent as a function of the relaxation time of $S(q,t)$ of lysozyme computed *without* the methyl-group hydrogen atoms.

temperature range studied which is limited by the thermal degradation of trehalose at high temperatures. Thus, the fact that we were able to collect data at high temperatures which are not experimentally accessible enabled us to detect the dynamical transition for the lysozyme-trehalose system. Furthermore, we find that the onset of the anharmonic motions inherent in the protein dynamical transition is observed far below the T_g of trehalose, thus indicating that the relaxation of the protein in such a glass is extended over a much wider temperature range than a hydrated amorphous powder or proteins in glycerol.

Another important result of Fig. 1 is the mean-square displacement of the hydrogen atoms in trehalose. Our study detects the secondary relaxation process in trehalose that is activated in our time window at temperatures close to 300 K. Since this temperature is below the T_g of trehalose, translational motions of trehalose molecules cannot occur and the relaxation has to be related to a change in conformation. Interestingly, the T_d of lysozyme is above the onset of this secondary relaxation which implies that for large solvent molecules a change in conformation is enough to break the hydrogen bonds between the protein and the solvent, thus allowing the protein to begin to undergo the dynamical transition. This mechanism is different for small solvent molecules such as water.

The remarkable similarity of the intermediate scattering function and the dynamic structure factor for the solvent and the protein (Figs. 2 and 4) confirms that our study captures the dynamical coupling as well as the consequent dynamical transition. Our analyses revealed details about the microscopic nature of the coupling. The solvent dynamics is transferred to the protein via the hydrogen bond network at the protein-solvent interface as exhibited by the correlation between structural relaxation of lysozyme and the hydrogen bond network at the interface shown in Fig. 9. Even though the protein dynamics is coupled to the solvent dynamics, the surface atoms of the protein follow the solvent dynamics more readily than the core atoms, as shown in Fig. 6. On the other hand, the dynamics of the solvent molecules is also modified: trehalose has enhanced dynamics near the protein

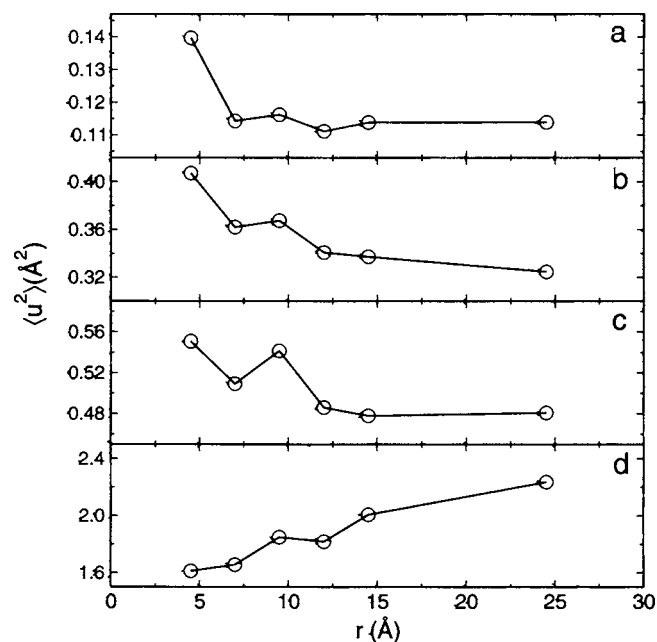


FIG. 10. Mean-square displacement of the hydrogen atoms in trehalose as a function of the distance from the surface of lysozyme at (a) 300, (b) 400, (c) 450, and (d) 550 K.

surface. This result contrasts the findings of previous studies of protein-solvent systems where it was reported that the dynamics of solvent molecules should be suppressed near the protein surface.

In order to clarify this observation and understand the relevance of this unexpected behavior on the dynamical coupling, we plotted $\langle u^2 \rangle$ as a function of the distance from the protein surface for a wide range of temperatures in Fig. 10. At temperatures below 450 K, $\langle u^2 \rangle$ decreases with increasing distance. This implies that trehalose molecules near the surface are more mobile than trehalose in the bulk. This behavior contradicts previous results on protein-glycerol and protein-water systems. However, as the temperature is increased from 300 to 450 K, Figs. 10(a)–10(c), the difference in the bulk to surface value of $\langle u^2 \rangle$ decreases from about 27% to 15%, suggesting that the effect becomes less pronounced. At 550 K the behavior reverses; trehalose becomes more mobile in the bulk than near the surface. Note that the glass transition temperature for trehalose as predicted by MD simulations is ~ 460 K.²⁷ Thus, at temperatures below and near the T_g of trehalose the protein is more mobile (as measured by $\langle u^2 \rangle$). Under this condition in order to achieve the dynamical coupling, the dynamics of trehalose molecules near the surface adapt to the dynamics of the protein [Figs. 10(a)–10(c)]. When temperature is above T_g , trehalose becomes more mobile than the protein, Fig. 10(d). This forces trehalose to gradually reduce its dynamics as it approaches the surface of the protein. This is caused by the reduced dimensionality of the space and the interactions with the protein; situation observed in earlier studies of protein-solvent systems.^{45,46}

Our observation that the dynamics of the solvent at the protein surface is different from the dynamics of the bulk can be interpreted from a different perspective using the concept

of *local* viscosity of the medium surrounding the protein. The diffusivity is proportional to mean square displacement (MSD) if linear dependency of MSD on time is satisfied, while viscosity is inversely proportional to diffusivity according to Stokes-Einstein relationship. Therefore, the viscosity of a fluid should increase monotonically with decreasing MSD of the molecules. Following this argument, the enhanced dynamics of trehalose near the surface of the protein [Figs. 7 and 10(a)–10(c)] can be viewed as the protein being surrounded by a solvent with a lower viscosity than the bulk viscosity. Such a situation implies that the protein sees an effective local viscosity that is lower than the viscosity of bulk solvent. In fact, this explains why lysozyme is more mobile than trehalose at 200 K as illustrated by a faster decay of $S(q, t)$ for the protein atoms in Fig. 6(a). Despite 200 K being lower than the T_g of trehalose, trehalose molecules near the surface are more mobile than trehalose in the bulk, thus facilitating the conformational changes of the protein which, otherwise, would not be viable in an environment with bulk viscosity.

V. CONCLUSIONS

In this article we have studied the coupling between the dynamics of lysozyme and trehalose. We found that the solvent molecules control the protein dynamics over a wide temperature range via intermolecular hydrogen bonds as illustrated by the correlation between the structural relaxation time of the protein and the relaxation time of hydrogen bond network formed at the protein-solvent interface. The dynamics of the surface of the protein is coupled to the dynamics of the solvent through hydrogen bonds formed between the first shell of solvent molecules and the surface atoms of the protein. This coupling is transferred into the protein interior via intramolecular interactions. Yet, the effect of the solvent dynamics on the core is not as strong as on the surface.

Our analysis shows the initiation of a dynamical transition in lysozyme at temperatures far below the glass transition of trehalose. This suggests that translational motion of the solvent molecule is not required to activate the onset of anharmonic dynamics in the protein. Nevertheless, the activation of some secondary relaxation in the solvent is necessary for the onset of anharmonic motions of lysozyme in trehalose. Another unexpected observation is the enhanced dynamics of trehalose close to the protein surface, opposite to that observed for water near the surface of a protein. The enhanced dynamics near the protein surface when combined with the secondary relaxation of trehalose at 300 K facilitates the molecular motions of the protein to such a degree that the initiation of anharmonic motions in the protein occurs far below the glass transition temperature of the solvent.

ACKNOWLEDGMENTS

This material is based upon work supported by the National Science Foundation under Grants No. CHE-0132278 and No. DMR-0315388. Acknowledgment is also made to The Ohio Board of Regents, Action Fund (Grant No. R566)

for financial support. One of the authors (J.E.C.) acknowledges the support of the National Research Council. Another author (G.A.C.) acknowledges Dr. Cicerone for the experimental data used in Fig. 1.

- ¹J. H. Crowe, L. M. Crowe, and D. Chapman, *Science* **223**, 701 (1984).
- ²S. J. Hagen, J. Hofrichter, and W. A. Eaton, *Science* **269**, 959 (1995).
- ³D. S. Gottfried, E. S. Peterson, A. G. Sheikh, J. Wang, M. Yang, and J. M. Friedman, *J. Phys. Chem.* **100**, 12034 (1996).
- ⁴L. Cordone, M. Ferrand, E. Vitrano, and G. Zaccai, *Biophys. J.* **76**, 1043 (1999).
- ⁵L. Cordone, P. Galajda, E. Vitrano, A. Gassmann, A. Ostermann, and F. Parak, *Eur. Biophys. J.* **27**, 173 (1998).
- ⁶J. Schlichter, J. Friedrich, L. Herenyi, and J. Fidy, *Biophys. J.* **80**, 2011 (2001).
- ⁷G. M. Sastry and N. Agmon, *Biochemistry* **36**, 7097 (1997).
- ⁸T. Takano, *J. Mol. Biol.* **110**, 569 (1997).
- ⁹A. Ansari, J. Berendzen, S. F. Bowne, H. Frauenfelder, I. E. T. Iben, T. B. Sauke, E. Shyamsunder, and R. D. Young, *Proc. Natl. Acad. Sci. U.S.A.* **82**, 5000 (1985).
- ¹⁰A. R. Bizzarri and S. Cannistraro, *J. Phys. Chem. B* **106**, 6617 (2002).
- ¹¹H. Frauenfelder, G. A. Petsko, and D. Tsernoglou, *Nature (London)* **280**, 558 (1979).
- ¹²D. Vitkup, D. Ringe, G. A. Petsko, and M. Karplus, *Nat. Struct. Biol.* **7**, 34 (2000).
- ¹³W. Doster, S. Cusack, and W. Petry, *Nature (London)* **337**, 754 (1989).
- ¹⁴I. E. T. Iben, D. Braunstein, W. Doster *et al.*, *Phys. Rev. Lett.* **62**, 1916 (1989).
- ¹⁵C. Arcangeli, A. R. Bizzarri, and S. Cannistraro, *Chem. Phys. Lett.* **291**, 7 (1998).
- ¹⁶P. W. Fenimore, H. Frauenfelder, B. H. McMahon, and F. G. Parak, *Proc. Natl. Acad. Sci. U.S.A.* **99**, 16047 (2002).
- ¹⁷G. Caliskan, A. Kisliuk, and A. P. Sokolov, *J. Non-Cryst. Solids* **868**, 307 (2002).
- ¹⁸G. Caliskan, D. Mechtani, J. H. Roh, A. Kisliuk, A. P. Sokolov, S. Az-zam, M. T. Cicerone, S. Lin-Gibson, and I. Peral, *J. Chem. Phys.* **121**, 1978 (2004).
- ¹⁹M. Uritani, M. Takai, and K. Yoshinaga, *J. Biochem. (Tokyo)* **117**, 774 (1995).
- ²⁰J. H. Crowe, J. F. Carpenter, and L. M. Crowe, *Annu. Rev. Physiol.* **60**, 73 (1998).
- ²¹D. A. Case, D. A. Pearlman, J. W. Caldwell *et al.*, *AMBER 7*, University of California, San Francisco, 2002.
- ²²J. Wang, P. Cieplak, and P. A. Kollman, *J. Comput. Chem.* **21**, 1049 (2000).
- ²³J. Wang, R. M. Wolf, J. W. Caldwell, P. A. Kollman, and D. A. Case, *J. Comput. Chem.* **25**, 1157 (2004).
- ²⁴G. M. Brown, D. C. Rohrer, B. Berking, C. A. Beevers, R. O. Gould, and R. Simpson, *Acta Crystallogr., Sect. B: Struct. Crystallogr. Cryst. Chem.* **28**, 3145 (1972).
- ²⁵M. J. Frisch, G. W. Trucks, H. B. Schlegel *et al.*, *GAUSSIAN 03*, Revision A.1, Gaussian, Inc., Pittsburgh PA, 2003.
- ²⁶H. J. C. Berendsen, J. P. M. Postma, W. F. van Gunsteren, A. DiNola, and J. R. Haak, *J. Chem. Phys.* **81**, 3684 (1984).
- ²⁷T. E. Dirama, G. A. Carri, and A. P. Sokolov, *J. Chem. Phys.* **122**, 114505 (2005).
- ²⁸P. W. Fenimore, H. Frauenfelder, B. H. McMahon, and R. D. Young, *Proc. Natl. Acad. Sci. U.S.A.* **101**, 14408 (2004).
- ²⁹A. M. Tsai, D. A. Neumann, and L. N. Bell, *Biophys. J.* **79**, 2728 (2000).
- ³⁰M. T. Cicerone and C. L. Soles, *Biophys. J.* **86**, 3836 (2004).
- ³¹A. De Gusseme, L. Carpentier, J. F. Willart, and M. Descamps, *J. Phys. Chem. B* **107**, 10879 (2003).
- ³²M. Ferrand, A. J. Dianoux, W. Petry, and G. Zaccai, *Proc. Natl. Acad. Sci. U.S.A.* **90**, 9668 (1993).
- ³³H. Lichtenegger, W. Doster, T. Kleinert, A. Birk, B. Sepiol, and G. Vogl, *Biophys. J.* **76**, 414 (1999).
- ³⁴J. E. Curtis, M. Tarek, and D. J. Tobias, *J. Am. Chem. Soc.* **126**, 15928 (2004).
- ³⁵D. Beece, L. Eisenstein, H. Frauenfelder, D. Good, M. C. Marden, L. Reinisch, A. H. Reynolds, L. B. Sorensen, and K. T. Yue, *Biochemistry* **19**, 5147 (1980).
- ³⁶H. Frauenfelder, P. G. Wolynes, and R. H. Austin, *Rev. Mod. Phys.* **71**, S419 (1999); H. Frauenfelder and B. H. McMahon, *Ann. Phys.* **9**, 655 (2000).
- ³⁷A. Paciaroni, S. Cinelli, and G. Onori, *Biophys. J.* **83**, 1157 (2002).
- ³⁸H. Frauenfelder, P. W. Fenimore, and B. H. McMahon, *Biophys. Chem.* **98**, 35 (2002).
- ³⁹M. Tarek and D. J. Tobias, *Phys. Rev. Lett.* **88**, 138101 (2002).
- ⁴⁰A. R. Bizzarri, C. X. Wang, W. Z. Chen, and S. Cannistraro, *Chem. Phys.* **201**, 463 (1995).
- ⁴¹T. E. Dirama, G. A. Carri, and A. P. Sokolov, *J. Chem. Phys.* **122**, 244910 (2005).
- ⁴²J. H. Roh, V. N. Novikov, R. B. Gregory, J. E. Curtis, Z. Chwdhuri, and A. P. Sokolov, *Phys. Rev. Lett.* **95**, 038101 (2005).
- ⁴³A. P. Sokolov, *J. Phys.: Condens. Matter* **11**, A213 (1999).
- ⁴⁴I. Pócsik and M. Koós, *Solid State Commun.* **74**, 1253 (1990).
- ⁴⁵G. N. Phillips and B. M. Pettitt, *Protein Sci.* **4**, 149 (1995).
- ⁴⁶V. A. Makarov, M. Feig, B. K. Andrews, and M. Pettitt, *Biophys. J.* **75**, 150 (1998).
- ⁴⁷F. Merzel and J. C. Smith, *Proc. Natl. Acad. Sci. U.S.A.* **99**, 5378 (2002).
- ⁴⁸W. Doster and M. Settles, in *Hydration Processes in Biology*, Nato Science, Series A: Life Science, edited by M. C. Bellissent-Funel (IOS, Berlin, 1999), Vol. 305, pp. 177–191.
- ⁴⁹M. Mezei and J. Beveridge, *J. Chem. Phys.* **74**, 622 (1981).